# SUPPORTING INFORMATION

High turnover frequency of hydrogen evolution reaction on amorphous MoS$_2$ thin film directly grown by atomic layer deposition

Seokhee Shin,[†] Zhenyu Jin,[†] Do Hyun Kwon, Ranjith Bose and Yo-Sep Min*

Department of Chemical Engineering, Konkuk University, 120 Neungdong-Ro, Gwangjin-Gu, Seoul 143-701, Korea
e-mail: ysmin@konkuk.ac.kr

Preparation of working electrode with catalyst: After the ALD of MoS$_2$ on Au/Ti/Si substrate, the geometrical area of the catalytic film was defined with a Kapton tape as shown in Fig. S1. The specimen was connected to a metal wire using silver paste. During the electrochemical measurements, the defined area of the working electrode was immersed into the electrolyte solution.
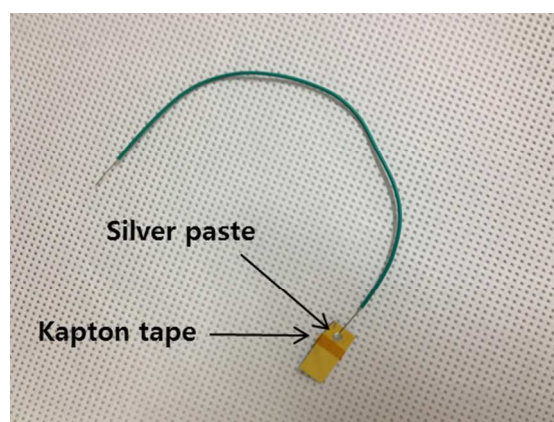

Figure S1. Picture of MoS$_2$/Au/Ti/Si working electrode of which the geometric area was defined to 1 cm^2 by a Kapton tape. The specimen was connected to a metal wire using silver paste.

Ohmic potential drop (iR) correction: The ohmic drop correction was performed with a series resistance (R_s) determined by electrochemical impedance measurement, according to the method given in Ref. S1. In our electrochemical setup, the series resistance may contain four components arising from the resistance in the wiring (R_{wiring}, e.g., electrode cables, alligator clips, Ag paste), the resistance in the Au substrate (R_{gold}), the solution resistance (R_{sol}) and the resistance due to the MoS_2 film itself (R_{film}). The electrochemical impedance measurements were performed at open circuit potential from 200 kHz to 50 mHz, using an AC amplitude of 25 mV. For all specimens, the series resistance was determined to be ~2.5 Ω by the real component of the impedance at high frequencies where the imaginary component is negligible, as shown in the Nyquist plot of Fig. S2. This reveals that the contribution of R_{film} to the series resistance is negligible. Therefore the iR correction using the measured R_s does not overestimate the HER activity. The experimental overpotential (η_{exp}) was corrected by subtracting the ohmic drop (iR_s) as the equation of $\eta_{corr} = \eta_{exp} - iR$.
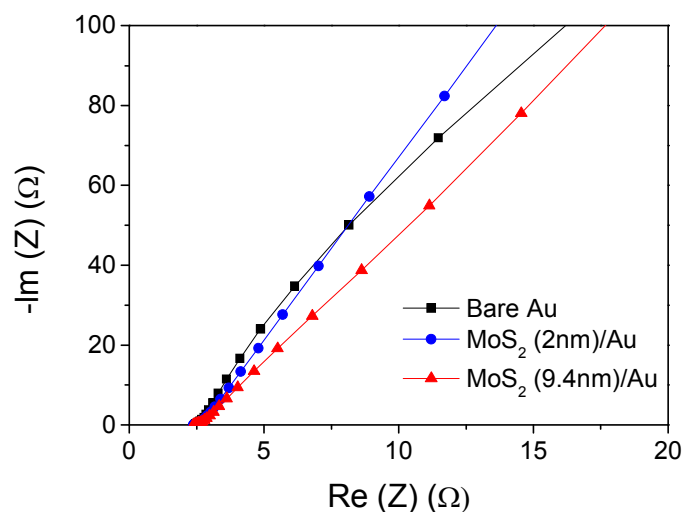

Figure S2. Nyquist plots of MoS_2 thin films and bare gold specimens performed at open circuit potential from 200 kHz to 50 mHz, using an AC amplitude of 25 mV. The series resistance was measured to be ~2.5 Ω for all specimens.

Capacitance measurements: Since the effective surface area of the catalyst film is linearly proportional to the double layer capacitance (C_{dl}), we performed cyclic voltammetry (CV) to obtain the values of C_{dl} for the MoS$_2$ films and the bare Au specimen in a potential range of 0.1 ~ 0.2 V with various scan rates (20, 40, 60, 80, 100 mV/s), according to the method in the Ref. S2. The cathodic (J_c) and anodic (J_a) current densities of the cyclic voltammograms in Figs. S3 (a-c) should be mainly originated from the charging of the electric double layer, because there is no faradaic process in the voltage range. In Fig. S3d, the current density difference (Δj) of J_c and J_a at 0.15 V vs RHE was plotted against the scan rate and fitted to a linear line. The slope represents a doubling of the double layer capacitance. The double layer capacitance of the bare Au, MoS$_2$ (2 nm)/Au, and MoS$_2$ (9.4 nm)/Au specimens are 8, 45, and 152 μF/cm^2, respectively. Comparing the double layer capacitances of the two MoS$_2$ specimens, the thinner film has a C_{dl} value 3.4 times smaller than the thicker film. This reveals that MoS$_2$ did not completely cover Au in the MoS$_2$ (2 nm)/Au specimen due to the ultrathin thickness.
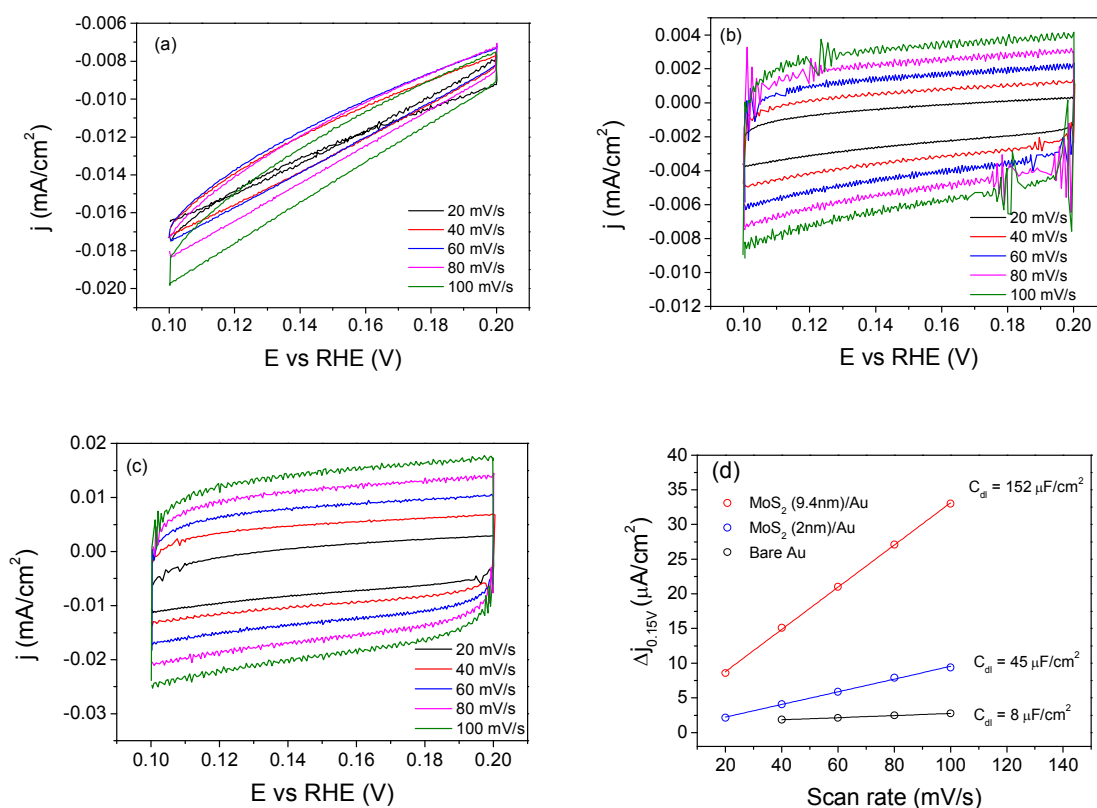

Figure S3. (a-c) Cyclic voltammograms in the range of 0.1 ~ 0.2 V vs RHE for the bare Au (a), MoS$_2$ (2 nm)/Au (b) and MoS$_2$ (9.4 nm)/Au (c) specimens. (d) The differences in current density ($\Delta j = j_a - j_c$) at 0.15 V vs RHE plotted against scan rate. The each plot was fitted to a linear line to determine the value of C_{dl}.

Grazing incidence X-ray reflectivity (XRR): For the MoS_2 film grown on a bare Si wafer, we performed low angle XRR measurement in the 2θ range of $0 \sim 2^o$ in order to obtain the film density. The experimental data was fitted for the film to be 12.8 nm with a density of 2.9 g/cm^3 as shown in Fig. S4. The thickness determined by XRR roughly agrees with the thickness (11.5 nm) determined by spectroscopic ellipsometer with a Tauc-Lorentz dispersion function.[S3] In addition, the density of the film reveals that the film is less dense in comparison to the crystalline MoS_2, due to the amorphous nature of the film grown at 100 ^{o}C.
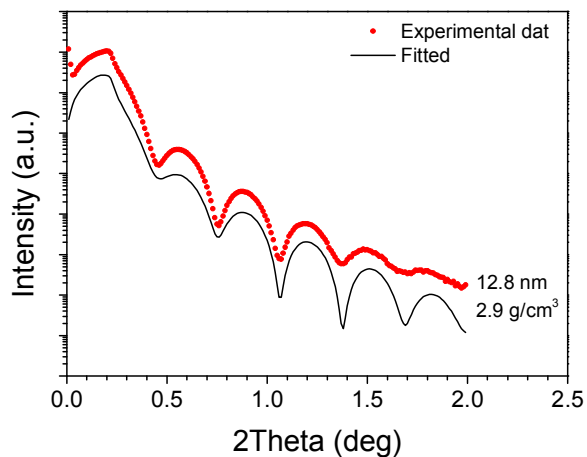

Figure S4. Low angle XRR data and its fitted curve for MoS_2/Si specimen.

Scanning electron microscopy (SEM) images: The high resolution SEM images were taken on the MoS$_2$ film grown on Au. For these images, any metal, which is generally coated on an insulating specimen to avoid the charging effect by electron beam, was not coated on the specimen, because the MoS$_2$ film is considerably conducting (Fig. 5). For the MoS$_2$ (2 nm)/Au, the grains of Au are clearly visible due to the ultrathin thickness. However the MoS$_2$ (9.4 nm)/Au specimen shows that the grains and their boundaries are covered by the film, even though the surface is still rough.
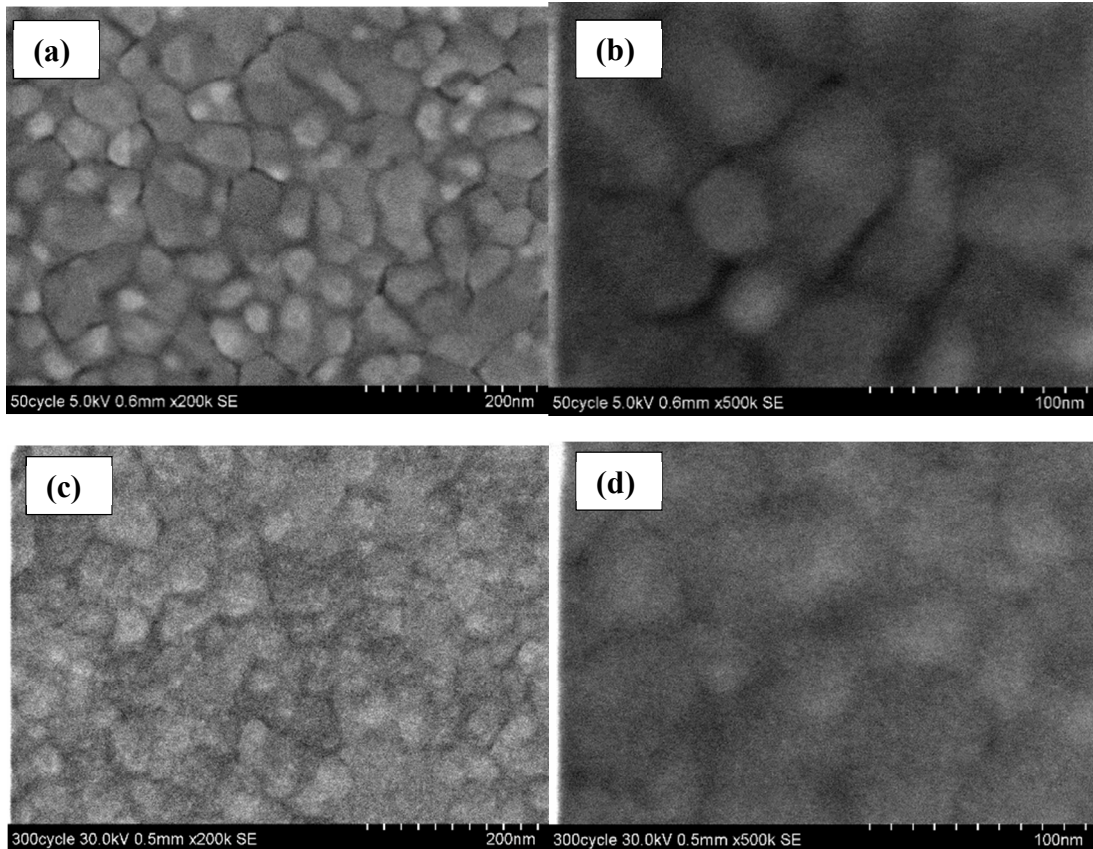
Figure S5. SEM images of MoS$_2$ (2 nm)/Au (a - b) and MoS$_2$ (9.4 nm)/Au (c - d).

Stability test of ALD-MoS$_2$ catalyst: For the stability test of the ALD-MoS$_2$/Au catalyst, the cyclic voltammetry (CV) was repeated for 1000 cycles between 0.205 ~ -0.195 V vs. RHE in 0.5 M H$_2$SO$_4$. There is a significant loss of activity after 1000 CV cycling.
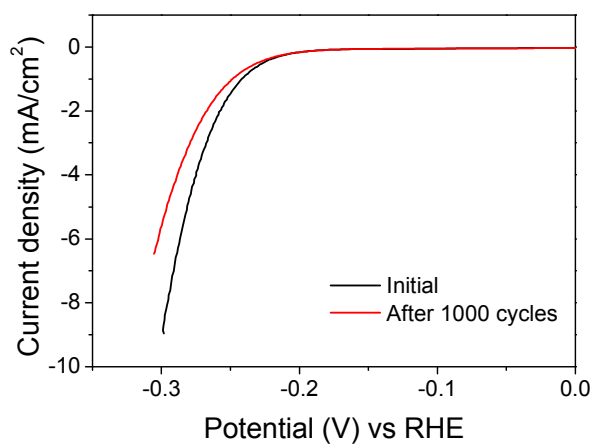
Figure S6. Stability of ALD-MoS$_2$/Au catalyst before and after 1000 CV cycling.

References

(S1) Chen, Z.; Cummins, D.; Reinecke, B. N.; Clark, E.; Sunkara, M. K; Jaramillo, T. F. *Nano Lett.* **2011**, 11, 4168.

(S2) Lukowski, M. A.; Daniel, A. S.; Meng, F.; Forticaux, A.; Li, L.; Jin, S. *J. Am. Chem. Soc.* **2013**, 135, 10274.

(S3) Yim, C.; O'Brien, M.; McEvoy, N.; Winters, S.; Mirza, I.; Lunney, J. G.; Duesberg, G. S. *Appl. Phys. Lett.* **2014**, 104, 103114.